

Th\_Dome4\_18

## The Apparent Anisotropy of the SEG-EAGE Overthrust Model

P. Cupillard<sup>1\*</sup>, W. Mulder<sup>2,3</sup>, P. Anquez<sup>1</sup>, A. Mazuyer<sup>1,4</sup>, J. Barthélémy<sup>5</sup>

<sup>1</sup> University of Lorraine; <sup>2</sup> Shell Global Solutions International B. V.; <sup>3</sup> Delft University of Technology; <sup>4</sup> Stanford University; <sup>5</sup> CEREMA

### Summary

The Earth interior contains heterogeneities at all scales, ranging from pores and mineral grains to major global units. On the contrary, seismic recordings only contain variations larger than the minimum wavelength  $\lambda_{\min}$ . The heterogeneities smaller than  $\lambda_{\min}$  are naturally smoothed by the wavefield, leading to effective media when inverting seismic recordings to image the Earth. In particular, oriented small-scale structures lead to apparent anisotropy. In the present work, we apply the non-periodic homogenization method to the SEG-EAGE overthrust model to get the effective properties of a typical subsurface medium and to estimate the magnitude and the symmetry of the apparent anisotropy. We show that such anisotropy can reach 18%, most of it being explained by locally-tilted transverse isotropy. We also show that using the effective properties within an anisotropic wave simulator considerably decreases the computation requirement with respect to a wave simulation in the original model.

## Introduction

The Earth interior contains heterogeneities at all scales, ranging from pores and mineral grains to major global units. On the contrary, seismic recordings only contain variations larger than the minimum wavelength  $\lambda_{min}$ . The heterogeneities smaller than  $\lambda_{min}$  are naturally smoothed by the wavefield, leading to effective media when inverting seismic recordings to image the Earth (Capdeville and Métivier, 2018). In particular, oriented small-scale structures lead to apparent anisotropy which is difficult to separate from the intrinsic one (Fichtner et al., 2013). Such apparent anisotropy illustrates the trade-off between the geological structures and the elastic properties in the seismic imaging problem (e.g. Prieux et al., 2011; Bodin et al., 2015).

In the context of horizontal layers, Backus (1962) first proposed an effective medium theory for seismic waves, showing that isotropic layers map into a smooth vertical transversely isotropic (VTI) medium. A more general theory that is able to handle any geometry of 2D and 3D structures within the Earth was developed by Capdeville et al. (2010); Guillot et al. (2010); Cupillard and Capdeville (2018). This theory is the non-periodic homogenization. It is able to provide the effective properties of any elastic medium for the seismic wave propagation in a given frequency band. In the present work we apply the non-periodic homogenization to the SEG-EAGE overthrust model in order to estimate the magnitude and the symmetry of the apparent anisotropy in a typical subsurface medium. We will show that i) locally-tilted transverse isotropy explains most of this anisotropy and ii) using the smooth effective medium within an anisotropic wave simulator considerably decreases the computation requirement with respect to a wave simulation in the original model.

## The non-periodic homogenization method

The non-periodic homogenization is a two-scale asymptotic method which derives from theories proposed in micromechanics in the 70's for computing effective properties of composite materials (e.g. Bensoussan et al., 1978). It has been developed in the context of seismic wave propagation to upscale the elasticity tensor  $\mathbf{C}$  of any earth model with no constraint on the shape, the size and the contrast of the heterogeneities (Capdeville et al., 2010; Guillot et al., 2010; Cupillard and Capdeville, 2018).

In practice, the non-periodic homogenization consists in

1. Solving the elastostatic equation

$$\nabla \cdot \left\{ \mathbf{C} : \left[ \mathbf{I} + \frac{1}{2}(\nabla \boldsymbol{\chi} + {}^t \nabla \boldsymbol{\chi}) \right] \right\} = \mathbf{0}, \quad (1)$$

where  $\mathbf{I}$  is the 4<sup>th</sup>-order identity tensor and  $\boldsymbol{\chi}$  is the solution of the equation. This solution can be seen as the static response of the medium to local unit strains.

2. Building the *strain concentrator*  $\mathbf{G}$  and the *stress concentrator*  $\mathbf{H}$  defined by

$$\mathbf{G} = \frac{1}{2}(\nabla \boldsymbol{\chi} + {}^t \nabla \boldsymbol{\chi}) + \mathbf{I} \quad \text{and} \quad \mathbf{H} = \mathbf{C} : \mathbf{G}, \quad (2)$$

where  $:$  is the tensor contraction  $[\mathbf{A} : \mathbf{B}]_{ijkl} = A_{ijmn} B_{mnkl}$ .

3. Low-pass filtering  $\mathbf{G}$  and  $\mathbf{H}$  to obtain the upscaled elasticity tensor  $\mathbf{C}^*$ :

$$\mathbf{C}^* = \mathcal{F}^{\lambda_{min}}(\mathbf{H}) : \mathcal{F}^{\lambda_{min}}(\mathbf{G})^{-1}. \quad (3)$$

To solve equation (1), we rely on a classic finite-element method (Cupillard and Capdeville, 2018), so we have to generate a mesh of the model we want to smooth. Figure 1 shows a tetrahedral mesh of the SEG-EAGE overthrust. Using degree-3 polynomials within this mesh, the finite-element method yields the two concentrators  $\mathbf{G}$  and  $\mathbf{H}$ . Then we choose  $\lambda_{min} = 200 \text{ m}$  (which corresponds to a maximum frequency of 8 Hz because the lowest S-wave velocity in the model is  $1600 \text{ m.s}^{-1}$ , ) to filter the concentrators. The obtained effective medium  $\mathbf{C}^*$  is shown in Figure 2.

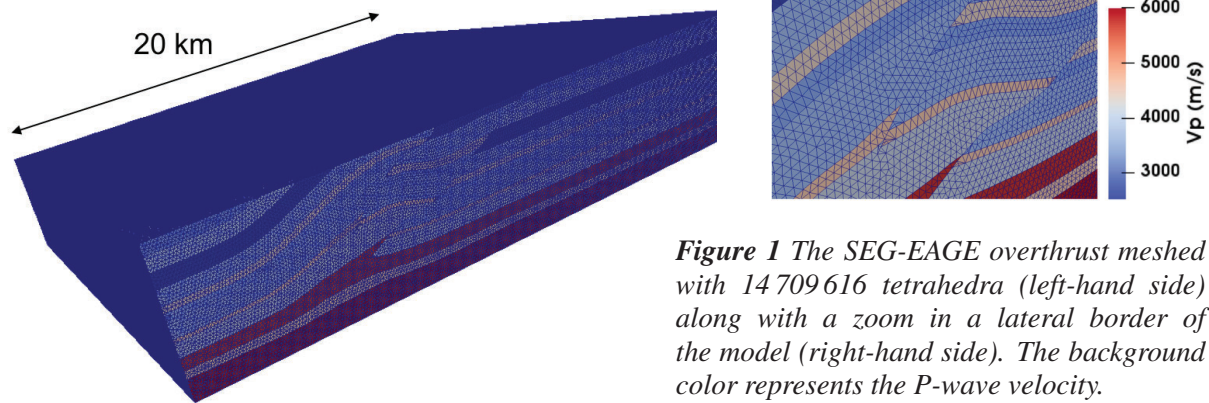


**Figure 1** The SEG-EAGE overthrust meshed with 14 709 616 tetrahedra (left-hand side) along with a zoom in a lateral border of the model (right-hand side). The background color represents the P-wave velocity.

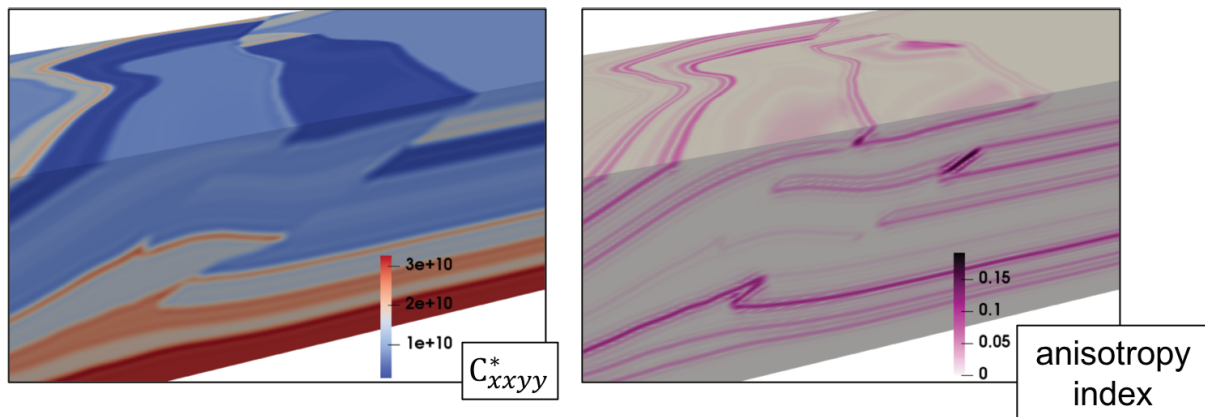


**Figure 2** The  $xxyy$ -component of the effective elasticity tensor  $\mathbf{C}^*$  of the SEG-EAGE overthrust model (left-hand side).  $\mathbf{C}^*$  is smooth; it does not contain scales smaller than  $\lambda_{\min} = 200\text{m}$ . Moreover, it is anisotropic (right-hand side) although the original model is isotropic.

### Analysis of the apparent anisotropy

Computing the distance of a given 4<sup>th</sup>-order tensor to the space of the isotropic tensors leads to the anisotropy index (e.g. Fedorov, 2013). This index quantifies the amount of anisotropy. When applied to  $\mathbf{C}^*$  at every point of the SEG-EAGE overthrust domain, we observe that the seismic anisotropy can reach 18 % (Figure 2). This anisotropy is purely apparent, as the original medium is isotropic.

To estimate how much some particular tensor symmetries explain this anisotropy, we compute the distance of  $\mathbf{C}^*$  to the space of both the transverse isotropic tensors and the orthotropic tensors in a basis with vertical and horizontal axis. Quite obviously, most of the anisotropy associated with sub-horizontal structures is VTI (Figure 3a). Strong anisotropy remains around tilted structures that the orthotropic symmetry is not able to explain (Figure 3b).

Figures 3c and 3d are similar to figures 3a and 3b, respectively. The difference is that we now locally optimize the basis in which the involved tensors are expressed. In other words, we look for the basis which minimizes the distance of  $\mathbf{C}^*$  to transverse isotropic and orthotropic tensors at every point in the domain. We observe that locally-tilted transverse isotropy explains all the amount of anisotropy almost everywhere (Figure 3c). At some particular locations where the velocity contrast is important and faults are involved, up to 3 % of anisotropy remains. This remaining anisotropy is not explained by the orthotropic symmetry (Figure 3d).

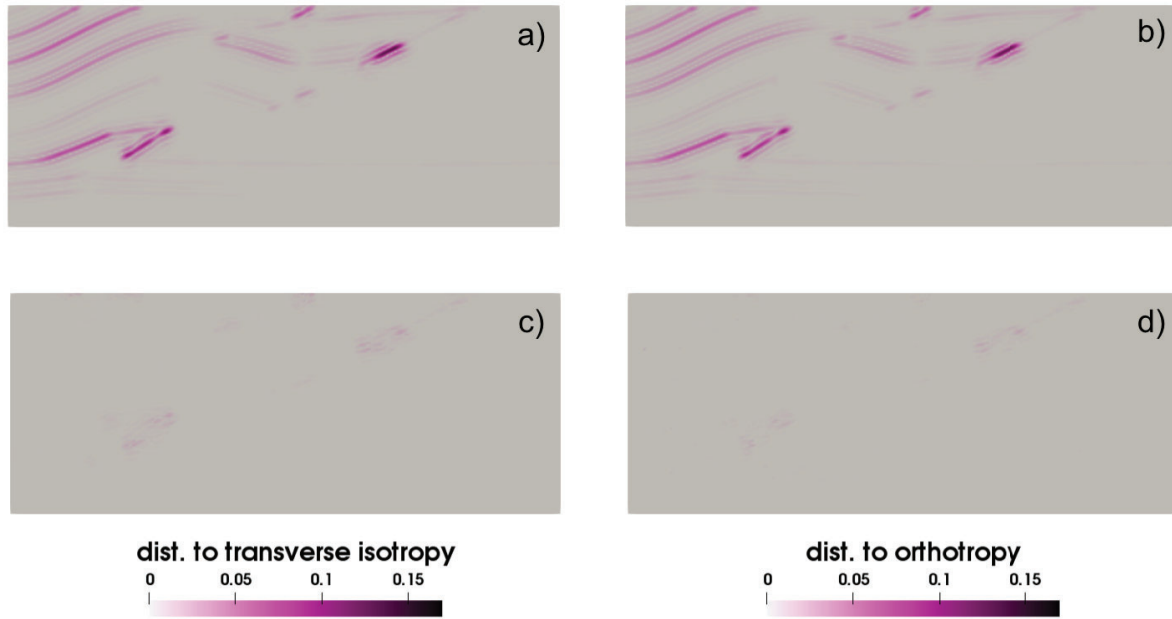


**Figure 3** Distance of the effective elasticity tensor  $C^*$  to the space of the transverse isotropic tensors (left-hand side) and to the space of the orthotropic tensors (right-hand side) in a basis with vertical and horizontal axis (top) and in an locally-optimized basis (bottom).

### Numerical simulations of wave propagation

To emphasize the relevance of the effective medium computed with the non-periodic homogenization, we perform a wave simulation in it and compare the result with a reference solution (Figure 4). Such a reference is obtained using a mass-lumped finite-element method (Geevers et al., 2019) on the tetrahedral mesh shown in figure 1. Because there are very small elements in this mesh to properly honor a couple of low-angle connections between faults and horizons, the computation requirement for the reference is enormous : 12.6 days on 40 cores to obtain 12 s seismograms. On the contrary, computing a wavefield in the effective medium is light because it is smooth so the mesh no longer has geological structures to honor. Here we use a simple hexahedral mesh (Figure 4a) to perform a spectral-element simulation (Cupillard et al., 2012) of the wavefield in the effective medium. The computation time for this simulation is 4 163 s, which is 260 times less than for the reference. As shown in figure 4b, the two wavefields match very well, the error averaged over 200 three-component stations being equal to 7.5 %.

### Conclusions

Based on the non-periodic homogenization of the SEG-EAGE overthrust model, we showed that apparent seismic anisotropy in the subsurface can be strong (up to 18 % in our case). Such anisotropy mixes with the intrinsic one in seismic data; in this context, the homogenization can be a useful tool to estimate potential apparent anisotropy and to put some error bars when interpreting intrinsic anisotropy.

Locally-tilted transverse isotropy explains most of the apparent anisotropy in our case. More complex cases (including fine-layering within units, oriented fractures, etc) would probably lead to more complex (e.g. tilted orthorhombic) anisotropy. In any case, looking for a low degree of symmetry in all the possible directions when inverting full waveforms (e.g. Warner et al., 2013) probably yields a homogenized medium. Assuming this, we can think of appraising structural earth models by comparing their homogenized equivalent medium to an anisotropic FWI model. That would allow testing structural scenarios, but further work on the relationship between FWI models and homogenized models has to be carried here (Capdeville and Métivier, 2018).

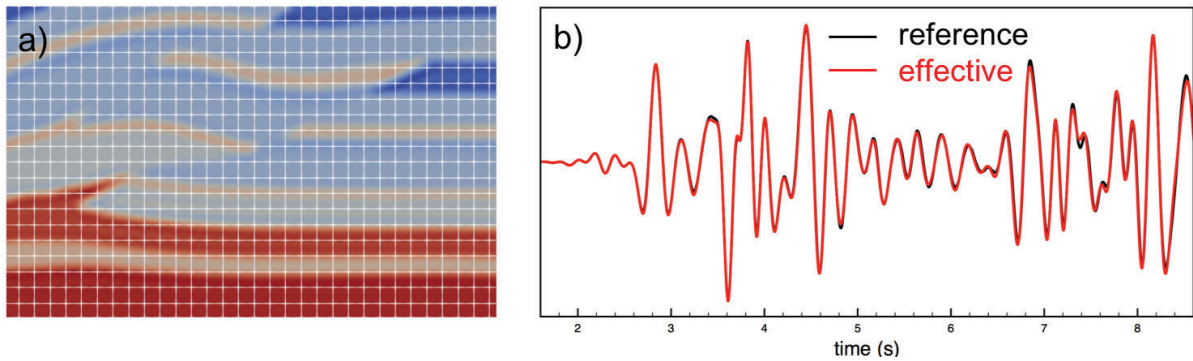


**Figure 4** A slice in a simple hexahedral mesh of the effective SEG-EAGE overthrust (left-hand side). The background color is the same as the one used in figure 2. A numerical simulation of wave propagation in this effective medium fits a reference simulation very well (right-hand side).

## Acknowledgements

We thank Albert Giraud for connecting P. Cupillard and J.-F. Barthélémy. We also thank RING-Gocad consortium ([www.ring-team.org](http://www.ring-team.org)) which has partially supported this work. Part of the calculations has been led on the EXPLOR centre hosted by the University of Lorraine.

## References

- Backus, G. [1962] Long-Wave Elastic Anisotropy Produced by Horizontal Layering. *J. Geophys. Res.*, **67**(11), 4427–4440.
- Bensoussan, A., Lions, J.L. and Papanicolaou, G. [1978] *Asymptotic Analysis of Periodic Structures*. North-Holland.
- Bodin, T., Capdeville, Y., Romanowicz, B. and Montagner, J.P. [2015] Interpreting radial anisotropy in global and regional tomographic models. In: *The Earth's Heterogeneous Mantle*, Springer, 105–144.
- Capdeville, Y., Guillot, L. and Marigo, J. [2010] 2-D non-periodic homogenization to upscale elastic media for P-SV waves. *Geophys. J. Int.*, **182**, 903–922.
- Capdeville, Y. and Métivier, L. [2018] Elastic full waveform inversion based on the homogenization method: theoretical framework and 2-D numerical illustrations. *Geophys. J. Int.*, **213**(2), 1093–1112.
- Cupillard, P. and Capdeville, Y. [2018] Non-periodic homogenization of 3-D elastic media for the seismic wave equation. *Geophys. J. Int.*, **213**(2), 983–1001.
- Cupillard, P., Delavaud, E., Burgos, G., Festa, G., Vilotte, J.P., Capdeville, Y. and Montagner, J.P. [2012] RegSEM: a versatile code based on the spectral element method to compute seismic wave propagation at the regional scale. *Geophys. J. Int.*, **188**, 1203–1220.
- Fedorov, F.I. [2013] *Theory of elastic waves in crystals*. Springer Science & Business Media.
- Fichtner, A., Kennett, B.L. and Trampert, J. [2013] Separating intrinsic and apparent anisotropy. *Phys. Earth Planet. Inter.*, **219**, 11–20.
- Geevers, S., Mulder, W.A. and van der Vegt, J.J. [2019] Efficient quadrature rules for computing the stiffness matrices of mass-lumped tetrahedral elements for linear wave problems. *SIAM journal on scientific computing*, **41**(2), A1041–A1065.
- Guillot, L., Capdeville, Y. and Marigo, J. [2010] 2-D non-periodic homogenization of the elastic wave equation: SH case. *Geophys. J. Int.*, **182**, 1438–1454.
- Prieux, V., Brossier, R., Gholami, Y., Operto, S., Virieux, J., Barkved, O.I. and Kommedal, J.H. [2011] On the footprint of anisotropy on isotropic full waveform inversion: the Valhall case study. *Geophys. J. Int.*, **187**(3), 1495–1515.
- Warner, M., Ratcliffe, A., Nangoo, T., Morgan, J., Umpleby, A., Shah, N., Vinje, V., Štekl, I., Guasch, L., Win, C. et al. [2013] Anisotropic 3D full-waveform inversion. *Geophysics*, **78**(2), R59–R80.